Spheroid-based 3-dimensional culture models: Gene expression and functionality in head and neck cancer

MARIANNE SCHMIDT[1], CLAUS-JUERGEN SCHOLZ[2], CHRISTINE POLEDNIK[1] and JEANETTE ROLLER[1]

[1]Department of Otorhinolaryngology, University of Würzburg, D-97080 Würzburg;
[2]Interdisciplinary Center for Clinical Research, Microarray Core Unit,
University of Würzburg, D-97078 Würzburg, Germany

Abstract. In the present study a panel of 12 head and neck cancer (HNSCC) cell lines were tested for spheroid formation. Since the size and morphology of spheroids is dependent on both cell adhesion and proliferation in the 3-dimensional (3D) context, morphology of HNSCC spheroids was related to expression of E-cadherin and the proliferation marker Ki67. In HNSCC cell lines the formation of tight regular spheroids was dependent on distinct E-cadherin expression levels in monolayer cultures, usually resulting in upregulation following aggregation into 3D structures. Cell lines expressing only low levels of E-cadherin in monolayers produced only loose cell clusters, frequently decreasing E-cadherin expression further upon aggregation. In these cell lines no epidermal growth factor receptor (EGFR) upregulation occurred and proliferation generally decreased in spheroids/aggregates independent of E-cadherin expression. In a second approach a global gene expression analysis of the larynx carcinoma cell line HLaC78 monolayer and the corresponding spheroids was performed. A global upregulation of gene expression in HLaC78 spheroids was related to genes involved in cell adhesion, cell junctions and cytochrome P450-mediated metabolism of xenobiotics. Downregulation was associated with genes controlling cell cycle, DNA-replication and DNA mismatch repair. Analyzing the expression of selected genes of each functional group in monolayer and spheroid cultures of all 12 cell lines revealed evidence for common gene expression shifts in genes controlling cell junctions, cell adhesion, cell cycle and DNA replication as well as genes involved in the cytochrome P450-mediated metabolism of xenobiotics.

Correspondence to: Dr Marianne Schmidt, Department of Otorhinolaryngology, University of Wuerzburg, Josef-Schneider-Strasse 11, D-97080 Wuerzburg, Germany
E-mail: schmidt_m2@ukw.de

Introduction

According to an analysis of over 3,000 cases of primary head and neck tumours in Germany in 2009, the patient benefit has not significantly improved from 1995 to 2006, despite new treatment strategies. Particularly, the 5-year overall survival rate for carcinomas of hypopharyngeal origin is very low with 27.2% (1). Hypopharyngeal cancer is often detected in later stages, since early signs and symptoms rarely occur. Late stages frequently involve multiple node affection, leading to poor prognosis (http://emedicine.medscape.com/article/1375268).

In vivo cells in a tissue context interact with neighbouring cells and extracellular matrix components. However, in 2-dimensional (2D) monolayer cultures cells tend to loose tissue-specific properties (2). 2D culture models therefore seem unsuitable to mimic the behaviour of cells in a natural, 3-dimensional (3D) microenvironment, particularly for testing of growth or invasion inhibiting substances, just as proposed in 1988 (3). In many aspects spheroids resemble the solid, non-vascularized tumour tissue and spheroidal cells show higher morphological and functional differentiation than monolayer cells. Upon proliferation of cells inside spheroids a tumour-like microenvironment develops with a hypoxic/necrotic core (reviewed in ref. 4), surrounded by quiescent and proliferating zones. Cells inside spheroids secrete extracellular matrix and functional cell junctions arise between cells, providing an advanced model system for examination of growth and invasion of carcinomas (4).

In the present study we compared the morphology and size of 12 HNSCC cell lines with the expression of the proliferation marker Ki67 and the cell-cell adhesion marker E-cadherin. Furthermore, the larynx carcinoma cell line HLaC78 was used as a model for comparing overall gene expression in 2D monolayer cultures with 72 h old HLaC78 multicellular spheroids. The results provide evidence for extensive restructuring of gene expression in the 3D context.

Materials and methods

Cell lines and cell culture. The cell lines used for spheroid analysis are listed in Table I. The cell lines were kept in RPMI-1640, 10% FCS and standard antibiotics, except Hep2 (MEM),

Table I. HNSCC cell lines used in the present study.

Cell line	Origin
FADU	Hypopharynx carcinoma, LGC standards (Wesel, Germany)
HLaC78	Larynx carcinoma (5)
Hep-2	Larynx carcinoma[a], LGC standards (Wesel, Germany)
Hep-2-Tax	Larynx carcinoma, paclitaxel-resistant clone
HLaC79	Larynx carcinoma (5)
HLaC79-Tax	Larynx carcinoma, paclitaxel-resistant clone
HPaC79	Parotis carcinoma (6)
HSmC78	Submandibular gland (5)
Cal27	Tongue, LGC standards (Wesel, Germany)
PE/CA-PJ41	Tongue, Sigma-Aldrich (Taufkirchen, Germany) (7)
SCC4	Tongue, LGC standards (Wesel, Germany)
HNO210	Larynx carcinoma, CLS (Eppelheim, Germany)

[a]Supposed to be HeLa contaminated, http://www.lgcstandards-atcc.org/products/all/CCL-23. HNSCC, head and neck cancer.

Hep2-Tax (MEM+20 μM paclitaxel), SCC4 [Dulbecco's modified Eagle's medium (DMEM/F12)] and HNO 210 (DMEM).

Spheroid formation. Tumour spheroids were generated by seeding 5,000 cells/well of Hep2 and Hep2-Tax cells in ultra-low attachment (ULA) 96-well round-bottomed plates (Corning, Amsterdam, The Netherlands) (8) or alternatively in ULA T75 flasks. Images were captured after 72 h with a Leica DMI 4000 inverted fluorescence microscope (Leica Microsystems, Wetzlar, Germany).

Expression micro array
RNA extraction and RNA quality control. RNA of HLaC78 monolayer and spheroidal cell cultures was isolated with the RNeasy kit (Qiagen, Hilden, Germany) according to the manufacturer's instructions. RNA quality was assessed with the RNA 6000 Nano kit using the Bioanalyzer 2100 instrument (Agilent, Böblingen, Germany). RNA integrity numbers (RINs) of our samples ranged between 9.4 and 9.9.

Microarray analysis. For microarray hybridization, 100 ng total RNA were amplified and labelled using the IVT Express kit and hybridized to GeneChip PrimeView Human Gene Expression arrays (both from Affymetrix, Santa Clara, CA, USA) according to the manufacturer's instructions.

Raw microarray data was background corrected, normalized and summarized to probe set expression values using the robust microarray average (RMA) [algorithm (9,10)]. Data preprocessing and calculation of $\log_2$ fold-changes between spheroid and monolayer expression values was performed in the R environment (http://www.r-project.org) using the Bioconductor (http://www.bioconductor.org) package 'affy'. Pathway enrichment analyses were performed with gene set enrichment analysis (GSEA) (11). Microarray data were deposited in MIAME-compliant form at Gene Expression Omnibus (http://www.ncbi.nlm.nih.gov/geo) with the identifier GSE67495.

Real-time PCR. Gene expression rates were determined by real-time TaqMan® PCR (Applied Biosystems, Foster City, CA, USA). RNA was isolated from cell lines and primary cells with the RNeasy kit according to the manufacturer's instructions. The High Capacity RNA-to-cDNA Master Mix (Applied Biosystems, Darmstadt, Germany) was used for cDNA reverse transcription. Real-time PCR was performed in triplicates on a Real-time PCR cycler (Applied Biosytems, Darmstadt, Germany) using the TaqMan® gene expression assays for E-cadherin (CDH1), N-cadherin (CDH2), Ki67 (MKI), gap junction protein β6 (GJB6), aldo-keto reductase family 1 member C1 (AKR1C1), cytochrome P450 1B1 (CYP1b1), flap endonuclease 1 (FEN1), mutL homolog 1 (MLH1), [replication factor C (activator 1) 3 (RFC3)], and epidermal growth factor receptor 1 (EGFR1).

Relative quantification was calculated according to the $2^{-\Delta\Delta Ct}$ method (12). Expression values were normalized to the expression of *GAPDH* as an endogenous control which proved to be expressed most stably throughout the cell lines.

Scanning electron microscopy. For examination of morphology of HLaC78 spheroidal surface SEM was performed. Spheroids were fixed overnight at 4˚C with 2% glutaraldehyde in 0.1 M phosphate-buffer. Subsequently, spheroids were treated with 2% osmiumtetroxide in 0.1 M phosphate-saccharose. After dehydration in graded ethanol series (35-100%), specimens were dried using a critical point dryer. Spheroids were then coated with carbon, sputtered with gold palladium particles and viewed with an SEM (DSM 962; Zeiss, Oberkochen, Germany).

Statistical analysis. All statistical analyses and graphs were performed with GraphPad Prism 4 (GraphPad Software, Inc., La Jolla, CA, USA).

Results

Morphology of spheroids and expression of crucial genes. Cells (5,000) of each cell line (Table I) were seeded into
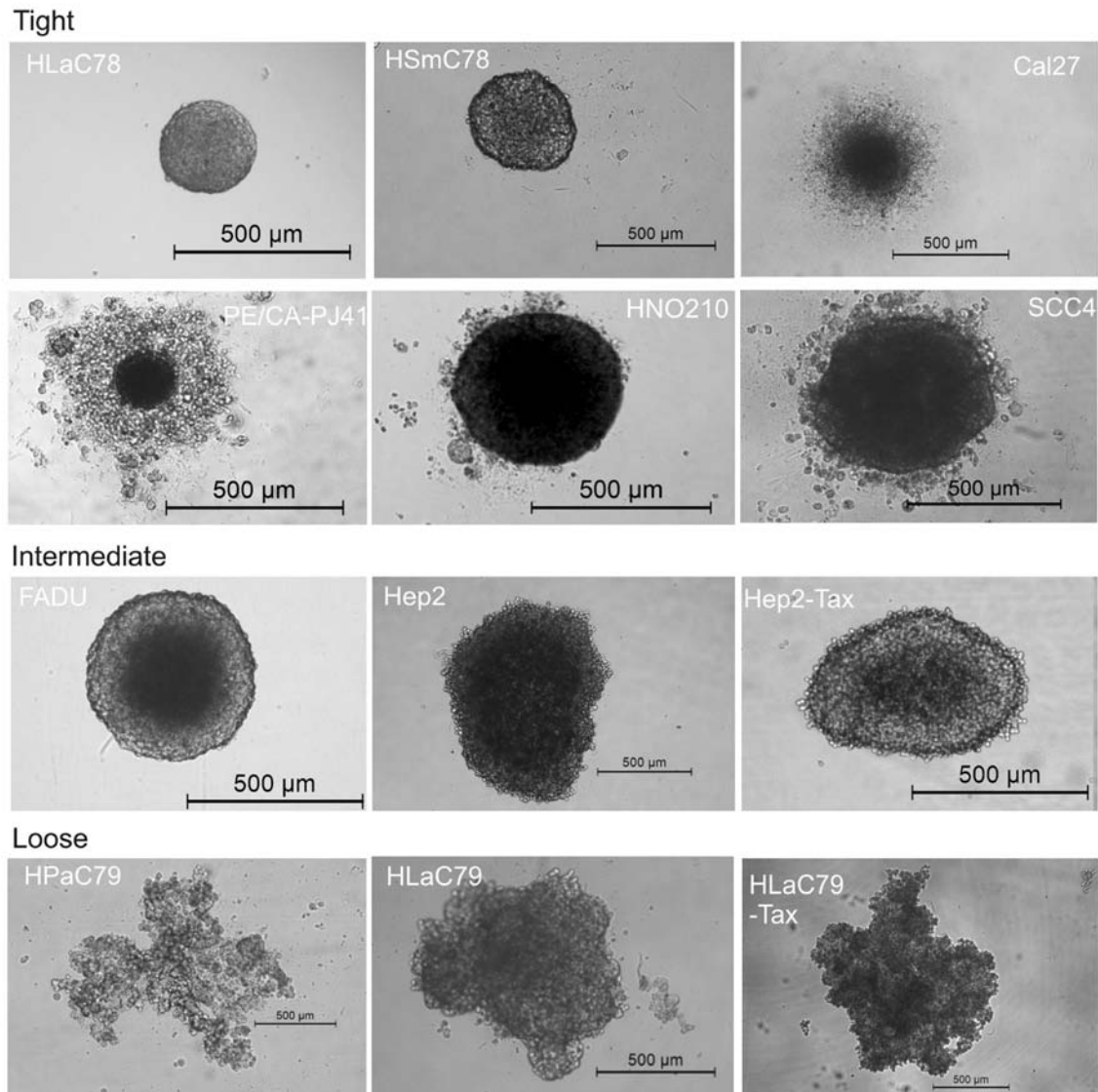
Figure 1. Spheroids of 10 different HNSCC cell lines established from 5,000 cells in ULA 96-well plates with conical bottom 72 h after seeding. Spheroids were grouped according to tightness.

96 ULA U-bottom well plates. Fig. 1 shows 72 h old spheroids originating from 5,000 cells of each cell line.

Fig. 1 demonstrates the morphological differences between spheroids of different monolayer origin. While HLaC78 and HSmC78 form small and very tight, nearly indestructible spheroids (even by harsh pipetting upon trypsin incubation), FADU, HNO210 and SCC-4 spheroids are larger in diameter, but also round shaped. Cal27 and PE/CA-PJ41 are typically surrounded by a halo of dead/non-aggregated cells. HPaC79, Hep2/Hep2-Tax and HLaC79/HLaC79-Tax cell lines rather aggregate into loose clusters. Spheroid size ranges from ~250 μm for tight, compact spheroids (HLaC78 and HsmC78) till diameters >1 mm (HPaC79).

In general spheroid sizes are both determined by tightness of cell-cell contacts and proliferation rates of the cell lines within the aggregates. Tightness of the spheroids and the proliferation rates within were measured by qRT-PCR expression analysis of E-cadherin (as a marker for adhesion)

and Ki67 (as a proliferation marker; Fig. 2) and opposed to expression of these markers in monolayers.

It is noticeable, that tight spheroids show either strong upregulation of E-cadherin upon aggregation (as HLaC78, zHSmC78 Cal27 or Pe/CA-PJ41). or a basic high E-cadherin expression in monolayer cultures with moderate increase/decrease (HNO210 and SSC4) following spheroid formation. Cell lines, agglomerating into intermediate or loose spheroids featured a basically low E-cadherin expression, increasing only weakly or decreasing upon loss of attachment to 2D surfaces (Fig. 2). Proliferation decreased in all cell lines except FADU, most markedly in cell lines forming tight spheroids. Since usually E-cadherin expression causes a decrease in proliferation (13) it is noticeable that the cell lines HPaC79, Hep2 and Hep2-Tax on the one hand decreased E-cadherin expression upon spheroid formation (log fold-changes HPaC79 -1.06, Hep2 -1.62, Hep2-Tax -2.20 and on the other hand also proliferation diminished (log fold-changes Ki67: HPaC79 -4.02, Hep2 -0.48 and Hep2-Tax -1.44; see
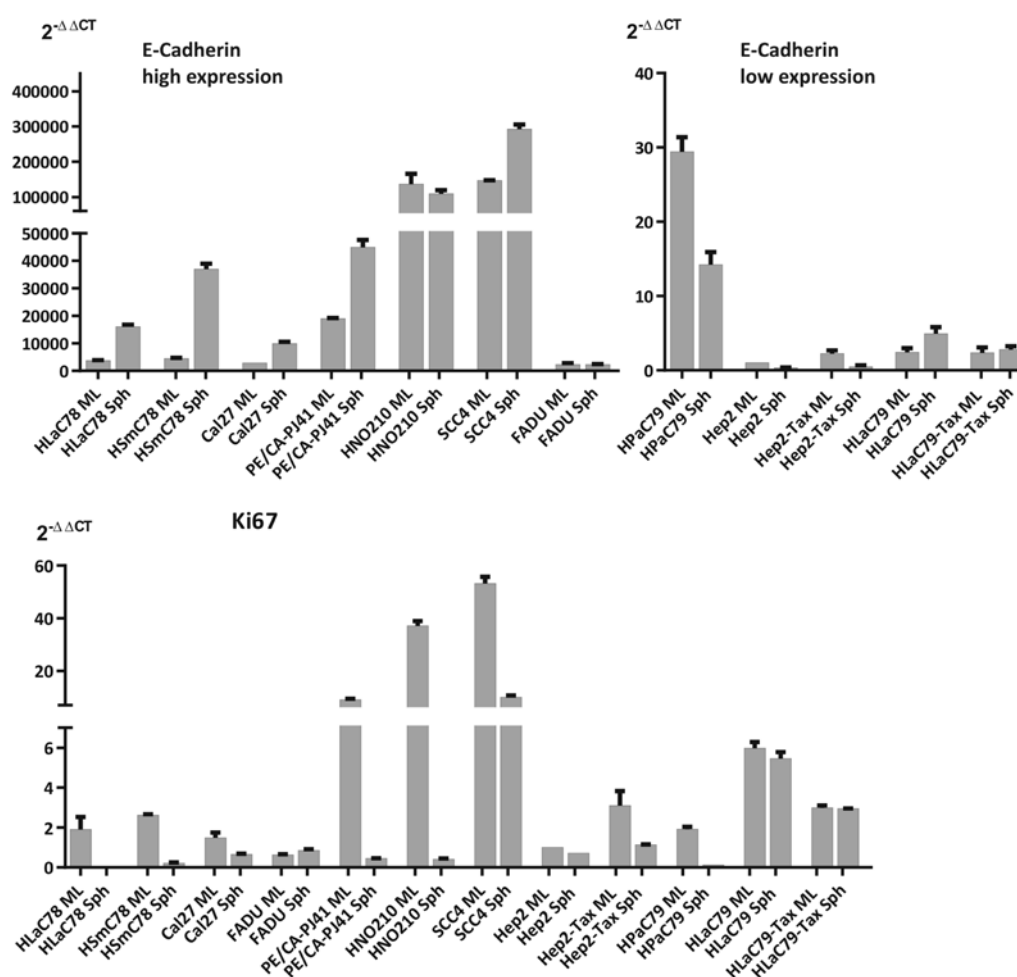
Figure 2. Expression of E-cadherin and Ki67 in monolayer cultures compared to spheroids of 12 different HNSCC cell line. For adequate presentation of E-cadherin cell lines were divided into groups expressing high or low levels of E-cadherin in monolayer cultures.

Table IV). Wang *et al* (14) described an enhancement of proliferation by downregulation of E-cadherin in HNSCC monolayer cell lines. The enhanced proliferation was mediated by upregulation of EGFR. To check this in the cell lines HPaC79, Hep2 and Hep2-Tax we performed qRT-PCR for EGFR. In these cell lines E-cadherin was downregulated along with EGFR in Hep2 (EGFR log fold-change -0.90) and Hep2-Tax (EGFR log fold-change 1.35) following aggregation. HPaC79 did not express EGFR in monolayer or in the spheroid culture.

Gene expression. Microarray analysis was used to create a gene expression array profile of head and neck cancer cell line growing as monolayer and in a 3D context. We selected the HLaC78 cell line due to its spontaneous aggregation into tight, well-shaped spheroids with a smooth, tissue-like surface with apical microvilli protrusions typical for epithelia (Fig. 3). A global upregulation of gene expression in HLaC78 larynx carcinoma cells line growing in a tissue-like 3D structure was primarily related to cell adhesion, cell junctions and cytochrome P450-mediated metabolism of xenobiotics. Expression downregulation could be predominantly associated with cell cycle, DNA replication and DNA mismatch repair.

A summary of selected differentially expressed probe sets is shown in Table II, subdivided into functional groups.

To transfer data obtained from HLaC78 expression analysis and to determine key changes in switching between 2D and 3D conditions, the expression of selected genes of each functional group were analyzed by quantitative RT-PCR in monolayer and spheroid cultures of 12 different HNSCC cell lines.

Genes selected for TaqMan® qRT-PCR expression quantification in monolayer and spheroid cultures of HNSCC cell lines are summarized in Table III, log fold-changes for spheroids of each cell line in comparison with monolayer culture are shown in Table IV.

Common expression shifts occurred in cell lines forming tight spheroids under 3D conditions. Thus, expression of cell junction and cell adhesion genes, as well as cytochrome P450 detoxification genes increased (GJB6, E-cadherin, AKR1C1, Cyp1a1 and 1b1), while expression of genes important for proliferation and DNA-replication (MKI and RCF3) decreased. In the DNA mismatch repair group no common tendency of expression shift was visibleX (at least for the tested FEN1/MLH1 genes). In cell lines, forming only loose aggregates, no upregulation of GJB6 or E-cadherin occurred under 3-dimensional conditions. Cell proliferation and DNA replication genes, however, were downregulated independent of spheroid compaction in the 3D context. Notably, the tested DNA mismatch repair genes were uniformly downregulated in cell lines aggregating loosely.

Table II. Log fold-changes in gene expression in spheroids vs. monolayer cultures of HLaC78 cell line.

Gene symbol	Gene	logFC
Cell junctions		
GJB6	Gap junction protein, β6, 30 kDa	4,588
CDH2	Cadherin 2, type 1, N-cadherin (neuronal)	-3,963
GJB2	Gap junction protein, β2, 26 kDa	3,547
CLDN10	Claudin 10	3,364
DSC2	Desmocollin 2	3,254
DSG3	Desmoglein 3	2,727
NOTCH3	Notch 3	2,723
GJA1	Gap junction protein, α1, 43 kDa	2,488
DSC3	Desmocollin 3	2,238
CLDN7	Claudin 7	2,222
NOTCH1	Notch 1	1,991
F11R	F11 receptor	1,887
CLDN8	Claudin 8	1,878
CAV1	Caveolin 1, caveolae protein, 22 kDa	-1,730
JUP	Junction plakoglobin	1,657
CDH1	Cadherin 1, type 1, E-cadherin (epithelial)	1,589
ITGB1	Integrin, β1 (fibronectin receptor)	-1,195
DSP	Desmoplakin	1,181
ITGB6	Integrin, β6	1,099
GJB5	Gap junction protein, β5, 31.1 kDa	1,041
Cell adhesion		
HLA-DRA	Major histocompatibility complex, class II, DRα	7,514
HLA-DRB1	Major histocompatibility complex, class II, DRβ1	4,842
HLA-DMA	Major histocompatibility complex, class II, DMα	4,692
HLA-DPA1	Major histocompatibility complex, class II, DPα1	4,391
HLA-F	Major histocompatibility complex, class I, F	4,050
HLA-DMB	Major histocompatibility complex, class II, Dβ	3,924
HLA-DRB5	Major histocompatibility complex, class II, DRβ5	3,864
HLA-DPB1	Major histocompatibility complex, class II, DPβ1	3,464
CLDN10	Claudin 10	3,364
HLA-B	Major histocompatibility complex, class I, B	2,965
HLA-C	Major histocompatibility complex, class I, C	2,618
HLA-DQB1	Major histocompatibility complex, class II, DQβ1	2,477
HLA-E	Major histocompatibility complex, class I, E	2,468
CLDN7	Claudin 7	2,222
PTPRM	Protein tyrosine phosphatase, receptor type, M	2,192
CD58	CD58 molecule	2,076
HLA-A	Major histocompatibility complex, class I, A	2,058
PVRL1	Poliovirus receptor-related 1 (herpesvirus entry mediator C)	2,016
F11R	F11 receptor	1,887
CLDN8	Claudin 8	1,878
CDH1	Cadherin 1, type 1, E-cadherin (epithelial)	1,589
CDH3	Cadherin 3, type 1, P-cadherin (placental)	1,566
NEO1	Neogenin 1	1,518
CD86	CD86 molecule	1,424
ITGB8	Integrin, β8	1,370
GLG1	Golgi glycoprotein 1	1,368
CNTN1	Contactin 1	1,366
CD40	CD40 molecule, TNF receptor superfamily member 5	1,359
SDC1	Syndecan 1	1,340
SDC2	Syndecan 2	1,265
PTPRF	Protein tyrosine phosphatase, receptor type, F	1,159
CD276	CD276 molecule	1,100

Table II. Continued.

Gene symbol	Gene	logFC
Cytochrome P450 metabolism		
AKR1C1	Aldo-keto reductase family 1, member C1	3,798
AKR1C3	Aldo-keto reductase family 1, member C3	3,364
CYP1B1	Cytochrome P450, family 1, subfamily B, polypeptide 1	2,837
CYP1A1	Cytochrome P450, family 1, subfamily A, polypeptide 1	2,327
GSTA4	Glutathione S-transferase α4	2,299
ALDH3B2	Aldehyde dehydrogenase 3 family, member B2	2,039
MGST2	Microsomal glutathione S-transferase 2	1,196
GSTK1	Glutathione S-transferase κ1	1,131
GSTZ1	Glutathione S-transferase ζ1	1,112
Cell cycle		
CDKN3	Cyclin-dependent kinase inhibitor 3	-5,795
CDK1	Cyclin-dependent kinase 1	-5,556
BIRC5	Baculoviral IAP repeat containing 5	-5,257
CCNA2	Cyclin A2	-5,205
CDC20	Cell division cycle 20 homolog (*S. cerevisiae*)	-5,19
CDC6	Cell division cycle 6 homolog (*S. cerevisiae*)	-5,104
MAD2L1	MAD2 mitotic arrest deficient-like 1 (yeast)	-4,665
CCNB1	Cyclin B1	-4,573
CDC25A	Cell division cycle 25 homolog A (*S. pombe*)	-4,500
AURKB	Aurora kinase B	-4,439
CCNB2	Cyclin B2	-4,387
MKI67	Antigen identified by monoclonal antibody Ki67	-4,028
BRCA1	Breast cancer 1, early onset	-3,798
RAD51	RAD51 homolog (*S. cerevisiae*)	-3,543
KNTC1	Kinetochore associated 1	-3,023
MCM3	Minichromosome maintenance complex component 3	-2,973
CKS2	CDC28 protein kinase regulatory subunit 2	-2,919
STMN1	Stathmin 1	-2,783
AURKA	Aurora kinase A	-2,778
GTSE1	G-2 and S-phase expressed 1	-2,719
CHEK1	Checkpoint kinase 1	-2,687
CKS1B	CDC28 protein kinase regulatory subunit 1B	-2,636
CCND2	Cyclin D2	-2,488
TFDP1	Transcription factor Dp-1	-2,242
BCCIP	BRCA2 and CDKN1A interacting protein	-2,239
TFDP1	Transcription factor Dp-1	-2,219
BRCA2	Breast cancer 2, early onset	-2,147
CDKN1A	Cyclin-dependent kinase inhibitor 1A (p21, Cip1)	2,116
CCNF	Cyclin F	-2,103
CDK2	Cyclin-dependent kinase 2	-1,949
RBL1	Retinoblastoma-like 1 (p107)	-1,905
SKP2	S-phase kinase-associated protein 2, E3 ubiquitin protein ligase	-1,580
MDM2	Mdm2, p53 E3 ubiquitin protein ligase homolog (mouse)	1,454
RAD1	RAD1 homolog (*S. pombe*)	-1,416
CCNE1	Cyclin E1	-1,379
CCNC	Cyclin C	-1,336
MAD2L2	MAD2 mitotic arrest deficient-like 2 (yeast)	-1,263
NBN	Nibrin	-1,249
CDK4	Cyclin-dependent kinase 4	-1,245
RB1	Retinoblastoma 1	-1,219
MCM4	Minichromosome maintenance complex component 4	-1,203
STMN1	Stathmin 1	-1,193
CDK5R1	Cyclin-dependent kinase 5, regulatory subunit 1 (p35)	-1,177

Table II. Continued.

| Gene symbol	Gene	logFC
CCNG2	Cyclin G2	1,102
CDK6	Cyclin-dependent kinase 6	-1,094
BCCIP	BRCA2 and CDKN1A interacting protein	-1,085
CCND1	Cyclin D1	-1,064
DNA mismatch repair		
FEN1	Flap structure-specific endonuclease 1	-2,869
NEIL3	Nei endonuclease VIII-like 3 (*E. coli*)	-2,787
POLE2	Polymerase (DNA directed), ε2, accessory subunit	-2,760
PCNA	Proliferating cell nuclear antigen	-2,279
HMGB1	High mobility group box 1	-2,076
PARP1	Poly(ADP-ribose) polymerase 1	-1,931
LIG1	Ligase I, DNA, ATP-dependent	-1,724
POLE	Polymerase (DNA directed), ε, catalytic subunit	-1,621
POLD3	Polymerase (DNA-directed), δ3, accessory subunit	-1,387
MBD4	Methyl-CpG binding domain protein 4	-1,378
MLH1	mutL homolog 1, colon cancer, non-polyposis type 2 (*E. coli*)	-1,369
POLD2	Polymerase (DNA directed), δ2, accessory subunit	-1,248
POLD1	Polymerase (DNA directed), δ1, catalytic subunit	-1,182
NEIL2	Nei endonuclease VIII-like 2 (*E. coli*)	-1,143
UNG	Uracil-DNA glycosylase	-1,132
DNA replication		
RFC3	Replication factor C (activator 1) 3, 38 kDa	-3,710
POLA2	Polymerase (DNA directed), α2, accessory subunit	-3,076
MCM3	Minichromosome maintenance complex component 3	-2,973
PRIM1	Primase, DNA, polypeptide 1 (49 kDa)	-2,948
FEN1	Flap structure-specific endonuclease 1	-2,869
MCM6	Minichromosome maintenance complex component 6	-2,859
MCM7	Minichromosome maintenance complex component 7	-2,853
POLE2	Polymerase (DNA directed), ε2, accessory subunit	-2,760
MCM4	Minichromosome maintenance complex component 4	-2,616
DNA2	DNA replication helicase/nuclease 2	-2,429
RNASEH2A	Ribonuclease H2, subunit A	-2,381
MCM2	Minichromosome maintenance complex component 2	-2,344
PCNA	Proliferating cell nuclear antigen	-2,279
RFC5	Replication factor C (activator 1) 5, 36.5 kDa	-2,227
RFC4	Replication factor C (activator 1) 4, 37 kDa	-2,086
RFC2	Replication factor C (activator 1) 2, 40 kDa	-1,798
LIG1	Ligase I, DNA, ATP-dependent	-1,724
POLA1	Polymerase (DNA directed), α1, catalytic subunit	-1,671
MCM5	Minichromosome maintenance complex component 5	-1,622
POLE	Polymerase (DNA directed), ε, catalytic subunit	-1,621
POLD3	Polymerase (DNA-directed), δ3, accessory subunit	-1,387
RPA3	Replication protein A3, 14 kDa	-1,368
RNASEH2B	Ribonuclease H2, subunit B	-1,260
POLD2	Polymerase (DNA directed), δ2, accessory subunit	-1,248
RFC1	Replication factor C (activator 1) 1, 145 kDa	-1,235
PRIM2	Primase, DNA, polypeptide 2 (58 kDa)	-1,185
POLD1	Polymerase (DNA directed), δ1, catalytic subunit	-1,182
POLE3	Polymerase (DNA directed), ε3, accessory subunit	-1,123
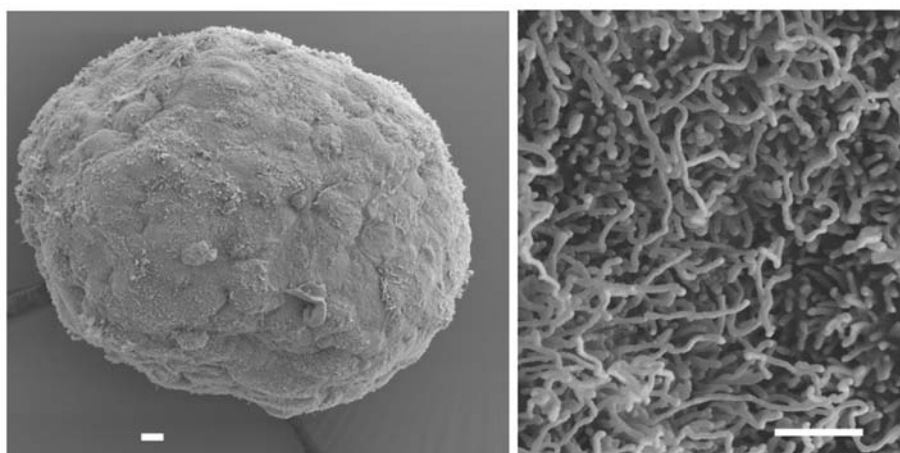
Figure 3. Scanning electron microscopy (SEM) display of a typical HLaC78 spheroid surface. Bar, 1 μm.

Table III. Genes tested for expression in monolayer and spheroid cultures of different HNSCC cell lines.

Functional group	Gene
Cell junctions	**GJB6**, gap junction protein β6
Cell adhesion	**CDH1**, E-cadherin
Cytochrome P450 metabolism	**AKR1C1**, aldo-keto family 1 reductase member
	CYP1B1, cytochrome P450 1B1
	CYP1A1, cytochrome P450 1A1
Cell cycle	**MKI**, Ki67 proliferative antigen
DNA mismatch repair	**FEN1**, flap endonuclease 1
DNA replication	**RFC3**, replication factor C3

HNSCC, head and neck cancer.

Discussion

The present study provides an overview of spheroid formation properties of 12 HNSCC cell lines. Spheroids differed enormously in size and tightness. The cell lines were divided in those forming tight spheroids or intermediate/loose aggregates. Since the size of spheroids is in general dictated by cell adhesion and proliferation rates within spheroids, expression profiles of Ki67 (proliferation) and E-cadherin (adhesion) were generated. For generation of tight, regular spheroids a distinct level of E-cadherin expression in monolayers was necessary and underwent a further significant upregulation upon aggregation. Alternatively, this further significant upregulation seemed to be expendable, when E-cadherin expression in monolayer cell lines was exceptionally high as in HNO210 or SCC4 cell lines, respectively. The cell lines expressing only low levels of E-cadherin under two-dimensional (2D) conditions were not able to gain a sufficient increase in E-cadherin expression to generate compact spheroidal tissue-like aggregates. Most of these cell lines even decreased E-cadherin expression under non-adherent conditions. Proliferation, however, decreased in all cell lines (except FADU) when the attachment to cell culture surfaces was suspended and 3-dimensional growth was initiated. The observation that spheroid tightness in HNSCC is partially determined by the expression of E-cadherin in monolayer culture is in agreement with the observation in other systems (15). In general upregulation of E-cadherin causes a β-catenin-ediated contact inhibition and subsequent decrease in proliferation (13). Furthermore, it has been shown that knock-down of E-cadherin enhances the proliferation of HNSCC cell lines by upregulating epidermal growth factor (EGFR) receptor. Despite the usual pathway of E-cadherin-mediated contact inhibition, in the cell lines HPaC78, Hep2 and Hep2-Tax, all forming only loose aggregates, E-cadherin was downregulated, but yet proliferation decreased. Obviously pathways initiated in monolayer cell cultures are not uniformly conferrable to the 3D context.

A comparison of overall gene expression between the monolayer culture of the human larynx carcinoma cell line HLaC78 and the corresponding 72 h old spheroids was performed. HLaC78 cells form tight spheroids spontaneously with a smooth, ciliated surface. Gene expression changed towards more tissue-like features. Changes in overall gene expression was organized in main functional groups, concerning cell junctions, cell adhesion, cytochrome P450 metabolism, cell cycle, DNA mismatch repair and DNA replication. While cell adhesion and cell junction gene expression increased, DNA replication/cell cycle genes as well as base excision DNA repair genes expression decreased in HLaC78 cell line. These principal observations roughly conform with a study on prostate cancer in 2007 (16), with respect to cell cycling, cell adhesion and DNA repair genes. In contrast, no angiogenesis genes were upregulated in HLaC78 upon spheroid aggregation, and vascular endothelial growth factor was slightly downregulated. It has to be considered, however, that in older spheroids an upregulation of angiogenesis genes may also occur, when central hypoxia increases (in the present study HIF-1 was upregulated only non-significantly after 72 h). To transfer data obtained from HLaC78 expression analysis line and to determine key changes in switching between 2D and 3D conditions, the expression of selected

Table IV. Log fold-changes in gene expression of selected genes in spheroids vs. monolayer cultures of HNSCC cell lines.

	GJB6	CDH1	AKR1C1	CYP1A1	CYP1B1	MKI	FEN1	MLH1	RCF3
Tight spheroids									
HLaC78	3.06	2.17	4.64	2.83	1.86	-5.55	-1.42	-0.37	-3.30
HSmC78	5.93	3.04	6.58	5.02	5.23	-3.71	0.73	0.81	-0.95
Cal27	5.05	1.81	4.04	4.69	2.55	-1.17	-0.22	1.34	-0.61
PE/CA-PJ41	0.49	1.35	2.76	6.78	4.88	-4.35	1.51	-0.04	-0.65
HNO210	5.75	-0.44	5.99	1.49	0.12	-6.48	3.31	0.40	-2.65
SCC4	0.59	0.79	0.15	5.71	0.75	-2.41	-0.92	0.91	-7.64
Loose/intermediate aggregates									
FADU	-0.68	0.06	0.04	0.45	0.79	0.43	-0.38	-0.52	-0.22
Hep2	-2.52	-1.62	-0.77	1.21	-2.21	-0.48	-1.85	-0.68	-1.57
Hep2-Tax	-2.23	-2.20	2.36	1.26	0.07	-1.44	-1.71	-3.17	-0.65
HPaC79	-1.16	-1.06	-1.27	-1.47	-3.89	-4.02	-1.56	-1.40	-5.58
HLaC79	-0.29	1.04	0.90	0.11	0.15	-0.13	-0.34	-1.09	-0.55
HLaC79-Tax	-5.22	-3.24	-7.64	-2.55	-0.99	-0.01	-5.95	-0.28	-0.68

HNSCC, head and neck cancer.

genes of each functional group were analyzed by quantitative RT-PCR in monolayer and spheroid cultures of different HNSCC cell lines.

The decrease in cell cycling/DNA synthesis seemed to be a common mechanism also in HNSCC cell lines, as shown by the expression analysis of Ki67 and RCF3. Cell junction and adhesion gene upregulation, however, was restricted to those cell lines with distinct E-cadherin expression already under two-dimensional conditions. These cell lines usually experienced a further upregulation of E-cadherin upon spheroid aggregation. Cell lines with low E-cadherin levels in monolayer cultures, however, further decreased expression under 3D conditions. This is somewhat divergent from the findings of Kim *et al* (17), who unveiled E-cadherin directly regulating the hippo signaling pathway controlling cell proliferation. E-cadherin mediates contact inhibition, which is essential for tissue maintenance. In the cell lines producing only loose aggregates, proliferation decreased despite downregulation of E-cadherin, indicating further pathways, regulating proliferation under tissue-like conditions.

Upregulation of cytochrome P450 metabolism genes has been solely reported several times for hepatocellular carcinoma cell lines. Thus, overall gene expression was analysed in HepG2 liver carcinoma monolayer cells and corresponding spheroids (18). The authors reported upregulation of cytochrome p450 1A1 (CYP1A1) as well as aldo-keto reductase C1 (AKR1C1), both factors involved in cytochrome P450-mediated metabolism of xenobiotics in spheroids. Hsiao *et al* (19) showed that CYP1A1 and CYP1B1 activity increased in hepatocytes with assembly of spheroids and decreased with disassembly of spheroids on collagen coated surfaces.

Notably, Masood *et al* (20) reported downregulation of CYP1A1 mRNA in head and neck cancer specimens compared to normal mucosal tissue. Upregulation of the cytochrome

P450 enzymes or AKR1A1 in spheroids may therefore reflect a regression to a more regulated cell type in a tissue-like context.

Francia *et al* (21) performed a differential display analysis of monolayers and spheroids of EMT-6 mammary carcinoma cells and compared differentially expressed genes with EMT-6 tumours selected *in vivo* to be resistant to alkylating agents. They identified the DNA mismatch repair-associated mismatch repair endonuclease 2 (PMS2) gene to be associated with resistance. Downregulation of PMS2 caused a multicellular resistance of tumour cell spheroids against alkylating agents. They hypothesized, that a deficiency in DNA mismatch repair may explain some forms of multicellular resistance, particularly to alkylating agents.

In HLaC78 genes of the functional group, DNA mismatch repair was significantly downregulated. We have not tested resistance of monolayers and spheroids of our cell lines against alkylating agents. Furthermore, it seems, that downregulation of DNA mismatch-repair genes is not a general mechanism of HNSCC cancer cell lines upon aggregation into spheroids, but it is notable, that the tested genes where more commonly downregulated in those cell lines forming loose clusters instead of tight spheroids.

Summarizing our results, it seems that in head and neck cancer cell lines (HNSCC) the 3D context reverses monolayer cells to growth and behavior of cells in a more tissue-like controlled condition with enhanced cell-cell adhesion and decreased proliferation. The formation of tight regular spheroids is dependent on distinct E-cadherin expression levels in monolayer cultures, usually resulting in further upregulation upon aggregation into 3D structures. Cell lines expressing only low levels of E-cadherin produce only loose cell clusters, frequently decreasing E-cadherin expression further. These cell lines diminish proliferation despite decreased E-cadherin. Common shifts in gene expression between 2D and 3D growth of HNSCC cell lines include the functional groups cell

junctions, cell adhesion, cell cycle, DNA replication as well as genes concerning the metabolism of xenobiotics.

References

1. Guntinas-Lichius O, Wendt T, Buentzel J, Esser D, Lochner P, Mueller A, Schultze-Mosgau S and Altendorf-Hofmann A: Head and neck cancer in Germany: A site-specific analysis of survival of the Thuringian cancer registration database. J Cancer Res Clin Oncol 136: 55-63, 2010.
2. Griffith LG and Swartz MA: Capturing complex 3D tissue physiology in vitro. Nat Rev Mol Cell Biol 7: 211-224, 2006.
3. Wustrow TP, Raffael A and Valet G: Multiparametric flow cytometry of human squamous cell carcinoma lines from the head and neck. Otolaryngol Head Neck Surg 98: 552-557, 1988.
4. Lin RZ and Chang HY: Recent advances in three-dimensional multicellular spheroid culture for biomedical research. Biotechnol J 3: 1172-1184, 2008.
5. Zenner HPLW, Lehner W and Herrmann IF: Establishment of carcinoma cell lines from larynx and submandibular gland. Arch Otorhinolaryngol 225: 269-277, 1979.
6. Zenner HP, Herrmann IF, Bremer W and Stahl-Maugé C: Head and neck carcinoma models. In vivo reproduction in athymic mice and in vitro culture. Acta Otolaryngol 95: 371-381, 1983.
7. Berndt A, Hyckel P, Könneker A, Katenkamp D and Kosmehl H: Oral squamous cell carcinoma invasion is associated with a laminin-5 matrix re-organization but independent of basement membrane and hemidesmosome formation. Clues from an in vitro invasion model. Invasion Metastasis 17: 251-258, 1997.
8. Vinci M, Gowan S, Boxall F, Patterson L, Zimmermann M, Court W, Lomas C, Mendiola M, Hardisson D and Eccles SA: Advances in establishment and analysis of three-dimensional tumor spheroid-based functional assays for target validation and drug evaluation. BMC Biol 10: 29, 2012.
9. Irizarry RA, Hobbs B, Collin F, Beazer-Barclay YD, Antonellis KJ, Scherf U and Speed TP: Exploration, normalization, and summaries of high density oligonucleotide array probe level data. Biostatistics 4: 249-264, 2003.
10. Bolstad BM, Irizarry RA, Astrand M and Speed TP: A comparison of normalization methods for high density oligonucleotide array data based on variance and bias. Bioinformatics 19: 185-193, 2003.
11. Subramanian A, Tamayo P, Mootha VK, Mukherjee S, Ebert BL, Gillette MA, Paulovich A, Pomeroy SL, Golub TR, Lander ES, *et al*: Gene set enrichment analysis: A knowledge-based approach for interpreting genome-wide expression profiles. Proc Natl Acad Sci USA 102: 15545-15550, 2005.
12. Livak KJ and Schmittgen TD: Analysis of relative gene expression data using real-time quantitative PCR and the $2^{-\Delta\Delta CT}$ method. Methods 25: 402-408, 2001.
13. Stockinger A, Eger A, Wolf J, Beug H and Foisner R: E-cadherin regulates cell growth by modulating proliferation-dependent beta-catenin transcriptional activity. J Cell Biol 154: 1185-1196, 2001.
14. Wang D, Su L, Huang D, Zhang H, Shin DM and Chen ZG: Downregulation of E-cadherin enhances proliferation of head and neck cancer through transcriptional regulation of EGFR. Mol Cancer 10: 116, 2011.
15. Ivascu A and Kubbies M: Diversity of cell-mediated adhesions in breast cancer spheroids. Int J Oncol 31: 1403-1413, 2007.
16. Takagi A, Watanabe M, Ishii Y, Morita J, Hirokawa Y, Matsuzaki T and Shiraishi T: Three-dimensional cellular spheroid formation provides human prostate tumor cells with tissue-like features. Anticancer Res 27: 45-53, 2007.
17. Kim NG, Koh E, Chen X and Gumbiner BM: E-cadherin mediates contact inhibition of proliferation through Hippo signaling-pathway components. Proc Natl Acad Sci USA 108: 11930-11935, 2011.
18. Chang TT and Hughes-Fulford M: Monolayer and spheroid culture of human liver hepatocellular carcinoma cell line cells demonstrate distinct global gene expression patterns and functional phenotypes. Tissue Eng Part A 15: 559-567, 2009.
19. Hsiao CC, Wu JR, Wu FJ, Ko WJ, Remmel RP and Hu WS: Receding cytochrome P450 activity in disassembling hepatocyte spheroids. Tissue Eng 5: 207-221, 1999.
20. Masood N, Malik FA and Kayani MA: Expression of xenobiotic metabolizing genes in head and neck cancer tissues. Asian Pac J Cancer Prev 12: 377-382, 2011.
21. Francia G, Man S, Teicher B, Grasso L and Kerbel RS: Gene expression analysis of tumor spheroids reveals a role for suppressed DNA mismatch repair in multicellular resistance to alkylating agents. Mol Cell Biol 24: 6837-6849, 2004.